2021 43rd Annual International Conference of the
IEEE Engineering in Medicine & Biology Society (EMBC)
Oct 31 - Nov 4, 2021. Virtual Conference

Inter-limb Asymmetry of Equilibrium Regulation in the Legs of 10–11-Year-Old Boys during Overground Sprinting

Kazuto Noro[1], *Student Member*, *IEEE*, Hiroaki Hirai[1], *Member*, *IEEE*,
Hideya Okamoto[2], Daisuke Kogawa[2], Chikako Kamimukai[2], Hiroshi Nagao[2], Yasunori Kaneko[2]
Kaito Hori[1], Satoru Yamamoto[1], Naoto Yamada[1], Takashi Yajima[1], Kazuhiro Matsui[1],
Atsushi Nishikawa[1], *Member*, *IEEE*, and Hermano Igo Krebs[3], *Fellow*, *IEEE*

***Abstract*— Short-distance running at top speed is important in field sports. Previous studies have analyzed kinematic and kinetic properties of sprinting in adults, but equivalent knowledge in children is underexplored. Quantifying relevant aspects of children's sprinting is useful for classifying their running skills and providing effective coaching based on motor control theory. This study aimed to clarify differences in equilibrium regulation in more- and less-skilled boy sprinters. Five 10–11-year-old boys regularly participating in lessons at the Mizuno running school performed 30-meter and 50-meter field track sprints, and the kinematic and electromyography findings were recorded. Equilibrium-point-based synergy analysis was then applied to estimate their respective virtual trajectories. The virtual trajectory is an equilibrium time sequence that indicates how the central nervous system controls a skeletal system with multiple muscles. The results suggested that: (1) the equilibrium of the right and left legs was regulated differently, although together the legs showed similar kinematics; (2) in the first type of virtual trajectory (type-I) in one leg, the equilibria after foot-strike were regulated intermittently during the early swing phase; (3) in the second type of virtual trajectory (type-II) in the other leg, the equilibria after foot-strike were continuously regulated during the early swing phase; and (4) the less-skilled child runners showed a slow equilibrium action response in both types of virtual trajectory during the early swing phase. These findings provide insights for "tailor-made" coaching based on the type of leg control during sprinting.**

***Clinical relevance*— Information on gait asymmetry would be beneficial not only for coaching to improve sprint training but also from clinical and injury perspectives.**

[1]Kazuto Noro, Hiroaki Hirai, Kaito Hori, Satoru Yamamoto, Naoto Yamada, Takashi Yajima, Kazuhiro Matsui, and Atsushi Nishikawa are with Department of Mechanical Science and Bioengineering, Graduate School of Engineering Science, Osaka University, Toyonaka, Japan {noro, hori, yamamoto, yamada, yajima}@hmc.me.es.osaka-u.ac.jp and {hirai, kmatsui, atsushi}@me.es.osaka-u.ac.jp

[2]Hideya Okamoto, Daisuke Kogawa, Chikako Kamimukai, Hiroshi Nagao, and Yasunori Kaneko are with Global Research and Development Department, Mizuno Corporation, Osaka, Japan {hokamoto, dkogawa, ckamimuk, hnagao, ykaneko}@mizuno.co.jp

[3]Hermano Igo Krebs is with Department of Mechanical Engineering, Massachusetts Institute of Technology, Cambridge, USA, Department of Neurology, University of Maryland, School of Medicine, Baltimore, USA, Department of Physical Medicine and Rehabilitation, Fujita Health University, Nagoya, Japan, Wolfson School of Engineering, Loughborough University, Loughborough, UK, Biomedical Engineering, University Campus Bio-Medico of Rome, Rome, Italy, Health Engineering Innovation Center, Khalifa University of Science and Technology, UAE, and Department of Mechanical Science and Bioengineering, Osaka University, Toyonaka, Japan hikrebs@mit.edu

I. INTRODUCTION

Top-speed short-distance running is often required in field sports. Previous studies have discussed factors determining motor skills during adult sprinting. Morin et al. (2012) reported that the main mechanical determinants of performance in 100-meter sprinting are (1) a "velocity-oriented" force-velocity profile, (2) a higher ability to convert ground reaction force to forward acceleration of the body, and (3) a higher step frequency resulting from a shorter contact time [1]. Dowson et al. (1998) reported that the relationship between isokinetic muscle strength and sprint performance during the acceleration phase relates to physique, such as limb length and body weight [2].

Although many studies have analyzed the kinematic and kinetic aspects of adult sprinting, scientific knowledge sprinting by children is underexplored. Children have different motor skills depending on their physique and ages. Among the few such studies, Schepens et al. (1998) and Mercer et al. (2010) studied body bounce and shock damping in sprinting children to elucidate the unique movement mechanism involved [3], [4]. Further, studies by Seki et al. (2016) on the kinematics of the swing in the legs of sprinting children indicated that increasing the swing speed was effective in improving performance [5]. However, these studies are limited to case reports. Quantifying equilibrium regulation in the leg muscles of sprinting children would be useful for classifying their running skills and providing effective coaching based on motor control theory.

This study aimed to understand the differences between skilled and less-skilled sprinting by 10–11-year-old boys

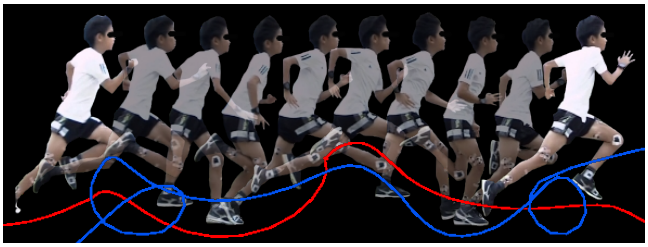

Fig. 1. Inter-limb asymmetry of the virtual trajectories during overground sprinting (representative participant A). The red and blue lines indicate the virtual trajectories for right and left legs, respectively. Cyclicity of the trajectories is evident in movement repeatability.

and to investigate equilibrium regulation via changes in muscle activity and kinematics during performance. A U.S.-patented synergy analyzer [6] was applied to estimate the equilibrium point (EP)-based co-activation synergies and the concomitant virtual trajectory in the configuration space. The virtual trajectory is defined as an equilibrium time sequence that indicates how the central nervous system controls a skeletal system with multiple muscles. Although this classic motor control problem [7] has not yet been solved, our results suggest that the equilibria are regulated differently for the right and left leg despite both legs showing similar kinematics (Fig. 1).

II. MATERIALS AND METHODS

A. Apparatus

Electromyography (EMG) data was gathered for the sprints described below from 16 electrodes on the lower limb muscles of both legs of each of the five participants. Data were recorded at 2000 Hz using wireless surface EMG sensors (PicoEMG, Cometa S.r.l., Italy) to measure the myoelectric potential of the following muscles: gluteus maximus (GM), iliopsoas (ILIO), semitendinosus (ST), rectus femoris (RF), vastus lateralis (VL), biceps femoris short head (BF), soleus (SOL), and tibialis anterior (TA) (Fig. 2(A) and Table I). The electrodes were secured on the skin surface over the bellies of the target muscles to minimize motion artifact and ensure signal quality [8], [9]. The raw EMG data were bandpass-filtered (fourth-order Butterworth filter, 20–450 Hz), rectified, outliers removed, and smoothed (fourth-order Butterworth filter, 10 Hz) before being normalized using the activity during maximum voluntary contraction (%MVC). The MVC level of each muscle was measured following standard procedures described in [10].

Kinematic data for 10 markers on the lower limbs were collected at 500 Hz using a high-speed camera (MEMRECAM Q1m, nac Image Technology Inc., Japan) to measure the hip, knee, ankle, heel, and toe positions in the sagittal plane.

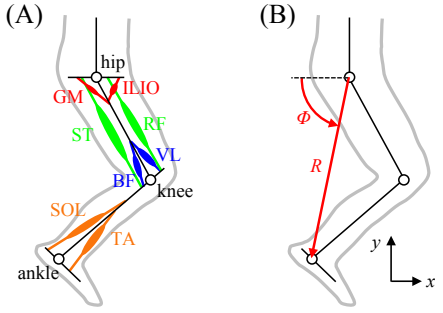

Fig. 2. Musculoskeletal model of the human lower limb. (A) Four pairs of agonist–antagonistic muscles around the hip, knee, and ankle joints. (B) Definition of endpoint position in two different coordinate systems: the space-fixed Cartesian coordinates (x, y) and the hip-centered polar coordinates (R, Φ).

B. Protocol

Five age-matched Japanese boys (all 10–11-years_old, 1.42 $\pm$ 0.05 m, 32.5 $\pm$ 6.95 kg) who regularly participate in running lessons at the Mizuno school were enrolled in the experiment. None of the participants reported any history of neuromuscular disorders or injuries. This study was approved by the Mizuno Corporation ethics committee. All participants provided their informed consent prior to inclusion.

After a brief introduction to the study and warm-up, the participants performed overground sprinting at an athletics field. Six 30-meter trials and one 50-meter trial were run with short breaks to prevent fatigue in the participants. The running performance of the participants was evaluated by an athletics instructor based on three measures of running (posture, arm action, and ground contact) on a five-point scale where 1=poor, 2=average, 3=good, 4=very good, and 5=excellent. The participants were then, classified into two groups: skilled (participants A, B, and C) and less-skilled (participants D and E) (TABLE II). As additional information for two groups, the 50-meter run times were 7.9 $\pm$ 0.1 seconds for the skilled group members and 9.1 $\pm$ 0.2 seconds for the less-skilled group members.

C. Analysis

Several gait cycles from near the midpoint (15-meter point) of the running track were focused on, and the corresponding data were used for the analysis of EMG and kinematics. A synergy analyzer [6] was used to estimate the EP-based co-activation synergies and the virtual trajectory in the configuration space of the EP-based co-activation synergies. The calculation procedure for the analysis can be summarized as:

1) Lower limb model: A human lower limb in the sagittal plane was modeled as a three-link limb with eight muscles (Fig. 2(A)). The eight muscles consisted of four pairs of

TABLE I
NAMES AND MOTOR FUNCTIONS OF TARGET MUSCLES

Label	Name	Motor function
Hip		
$m_{\mathrm{h,e}}$	Gluteus maximus (GM)	Hip extensor
$m_{\mathrm{h,f}}$	Iliopsoas (ILIO)	Hip flexor
Hip and knee		
$m_{\mathrm{hk,e}}$	Semitendinosus (ST)	Hip extensor and knee flexor
$m_{\mathrm{hk,f}}$	Rectus femoris (RF)	Hip flexor and knee extensor
Knee		
$m_{\mathrm{k,e}}$	Vastus lateralis (VL)	Knee extensor
$m_{\mathrm{k,f}}$	Biceps femoris short head (BF)	Knee flexor
Ankle		
$m_{\mathrm{a,e}}$	Soleus (SOL)	Ankle planterflexor
$m_{\mathrm{a,f}}$	Tibialis anterior (TA)	Ankle dorsiflexor

TABLE II
RUNNING PERFORMANCE EVALUATION BY ATHLETICS INSTRUCTOR

Participant	Posture	Arm action	Ground contact	Total score
A	4	4	4	4
B	4	4	4	4
C	4	3	4	4
D	3	2	3	3
E	2	2	3	2

TABLE III
DEFINITION OF THE A-A RATIO AND A-A SUM PARAMETERS

Label	Definition	Motor function
A-A ratio		
r_{h}	$m_{\mathrm{h,e}}/(m_{\mathrm{h,e}}+m_{\mathrm{h,f}})$	Hip extention index
r_{hk}	$m_{\mathrm{hk,e}}/(m_{\mathrm{hk,e}}+m_{\mathrm{hk,f}})$	Hip extention and knee flexion index
r_{k}	$m_{\mathrm{k,e}}/(m_{\mathrm{k,e}}+m_{\mathrm{k,f}})$	Knee extention index
r_{a}	$m_{\mathrm{a,e}}/(m_{\mathrm{a,e}}+m_{\mathrm{a,f}})$	Ankle plantar flexion index
A-A sum		
s_{h}	$m_{\mathrm{h,e}}+m_{\mathrm{h,f}}$	Hip stiffness index
s_{hk}	$m_{\mathrm{hk,e}}+m_{\mathrm{hk,f}}$	Hip and knee stiffness index
s_{k}	$m_{\mathrm{k,e}}+m_{\mathrm{k,f}}$	Knee stiffness index
s_{a}	$m_{\mathrm{a,e}}+m_{\mathrm{a,f}}$	Ankle stiffness index

agonist–antagonist (A-A) muscles around the hip, knee, and ankle joints. The activity of each muscle was normalized for the activity during MVC. Table I lists the names and motor functions of the target muscles. The endpoint movement was described by space-fixed Cartesian coordinates (x, y) or hip-centered polar coordinates (R, Φ) (Fig. 2(B)).

2) EP-based co-activation synergies and virtual trajectory: The EP-based co-activation synergy is a hypothetical concept of muscle coordination, which is derived from the physical model of equilibrium at the endpoint. The organized muscle activity can be explained by the theoretical values of antagonistic muscle pairs: the A-A ratio (quantity related to the equilibrium joint angle) and the A-A sum (a quantity associated with the joint stiffness). Theoretical and experimental studies support this concept [11], [12], [13], [14], [15]. The A-A ratio and A-A sum are defined as follows:

$$r_{\mathrm{j}} = \frac{m_{\mathrm{j,e}}}{m_{\mathrm{j,e}}+m_{\mathrm{j,f}}} \quad (1)$$

$$s_{\mathrm{j}} = m_{\mathrm{j,e}}+m_{\mathrm{j,f}} \quad (2)$$

where $m_{\mathrm{j,e}}$ and $m_{\mathrm{j,f}}$ denote the EMG activity of the extensor and flexor muscles at joint j (j = h [hip], hk [hip and knee], k [knee], a [ankle]), respectively. TABLE III shows the A-A ratios and A-A sums and their functions for the lower limb. The equilibrium of endpoint movement (R_{EP}, Φ_{EP}) can be expressed as a function of the A-A ratios and A-A sums. Equilibrium:

$$R_{\mathrm{EP}} = C_R \Delta w_R + \overline{R}_{\mathrm{EP}} \quad (3)$$

$$\Phi_{\mathrm{EP}} = C_\Phi \Delta w_\Phi + \overline{\Phi}_{\mathrm{EP}} \quad (4)$$

Synergy activation coefficients:

$$\begin{bmatrix}\Delta w_R \\ \Delta w_\Phi\end{bmatrix} = \begin{bmatrix}\boldsymbol{u}_R{}^T \\ \boldsymbol{u}_\Phi{}^T\end{bmatrix} \begin{bmatrix}\Delta r_{\mathrm{h}} \\ \Delta r_{\mathrm{hk}} \\ \Delta r_{\mathrm{k}}\end{bmatrix} \quad (5)$$

EP-based co-activation synergies:

$$\boldsymbol{u}_R = \frac{\boldsymbol{q}_2}{|\boldsymbol{q}_2|} \quad (6)$$

$$\boldsymbol{u}_\Phi = \frac{\boldsymbol{q}_1 - \frac{1}{2}\boldsymbol{q}_2}{|\boldsymbol{q}_1 - \frac{1}{2}\boldsymbol{q}_2|} \quad (7)$$

$$\boldsymbol{u}_{null} = \boldsymbol{u}_R \times \boldsymbol{u}_\Phi \quad (8)$$

$$\boldsymbol{q}_1 = \frac{1}{s_{\mathrm{h}}s_{\mathrm{hk}} + s_{\mathrm{hk}}s_{\mathrm{k}} + s_{\mathrm{k}}s_{\mathrm{h}}} \begin{bmatrix} -s_{\mathrm{h}}s_{\mathrm{hk}} - s_{\mathrm{k}}s_{\mathrm{h}} \\ -s_{\mathrm{hk}}s_{\mathrm{k}} \\ -s_{\mathrm{hk}}s_{\mathrm{k}} \end{bmatrix} \quad (9)$$

$$\boldsymbol{q}_2 = \frac{1}{s_{\mathrm{h}}s_{\mathrm{hk}} + s_{\mathrm{hk}}s_{\mathrm{k}} + s_{\mathrm{k}}s_{\mathrm{h}}} \begin{bmatrix} -s_{\mathrm{h}}s_{\mathrm{hk}} \\ s_{\mathrm{h}}s_{\mathrm{hk}} \\ -s_{\mathrm{hk}}s_{\mathrm{k}} - s_{\mathrm{k}}s_{\mathrm{h}} \end{bmatrix} \quad (10)$$

where C_R and C_Φ are the gains, $\overline{R}_{\mathrm{EP}}$ and $\overline{\Phi}_{\mathrm{EP}}$ are the mean values, Δw_R and Δw_Φ are the synergy activation coefficients, and $\boldsymbol{u}_R$, $\boldsymbol{u}_\Phi$, and $\boldsymbol{u}_{null}$ are the EP-based co-activation synergies. The suffixes R and Φ denote the radial and tangential directions, respectively, in the hip-centered polar coordinates. Furthermore, $null$ denotes null space. The EP-based co-activation synergy is the base unit vector that represents the equilibrium of endpoint movement in each direction (R, Φ, and $null$). The synergy activation coefficient represents the magnitude of the corresponding co-activation synergy. The EP-based co-activation synergy $\boldsymbol{u}_R$ and synergy activation coefficient Δw_R contribute to lifting of the endpoint, while the EP-based co-activation synergy $\boldsymbol{u}_\Phi$ and synergy activation coefficient Δw_Φ contribute to the forward movement of the endpoint. The EP-based co-activation synergy $\boldsymbol{u}_{null}$ does not contribute to the endpoint motion directly but contributes to the modification of the mechanical impedance at the endpoint. The EP-based co-activation synergy is a function of A-A sums only, and the synergy activation coefficient is a function of A-A ratios and A-A sums. The virtual trajectory is a time sequence of the equilibrium; that is, $R_{\mathrm{EP}}(t)$ and $\Phi_{\mathrm{EP}}(t)$, along time t. More details can be found in [11], [12], [13].

III. RESULTS

A. EP-based co-activation synergies

Figure 3 shows the EP-based co-activation synergies $\boldsymbol{u}_R$ (circle), $\boldsymbol{u}_\Phi$ (triangle), and $\boldsymbol{u}_{null}$ (square) in both legs during sprinting by participants. The filled and open markers

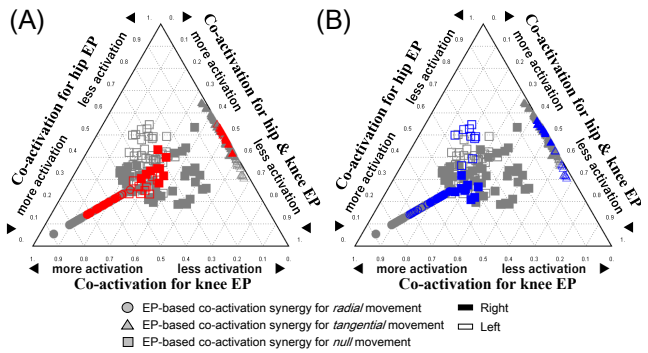

Fig. 3. EP-based co-activation synergies in sprinting by children. The red markers in (A) indicate the EP-based co-activation synergies of a skilled child runner (representative participant A), the blue markers in (B) indicate the EP-based co-activation synergies of a less-skilled runner (representative participant D), and the gray markers in each figure indicate the EP-based co-activation synergies of the other participants. All participants showed a similar distribution of EP-based co-activation synergies for radial (circle markers), tangential (triangle markers), and null (square markers) movement, regardless of the skilled or less-skilled classification.

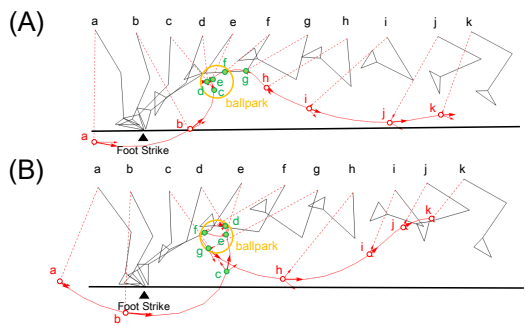

Fig. 4. Type-I virtual trajectory and kinematic posture. (A) a skilled child runner (representative participant A) and (B) a less-skilled child runner (representative participant D). The thick arrow along the virtual trajectory indicates the equilibrium velocity and the thin arrows indicate its radial and tangential components in the hip-centered polar coordinates. The equilibria after foot-strike were regulated intermittently, moving to a ballpark with a high velocity. The less-skilled child runner showed a relatively slow equilibrium action response during the early swing phase.

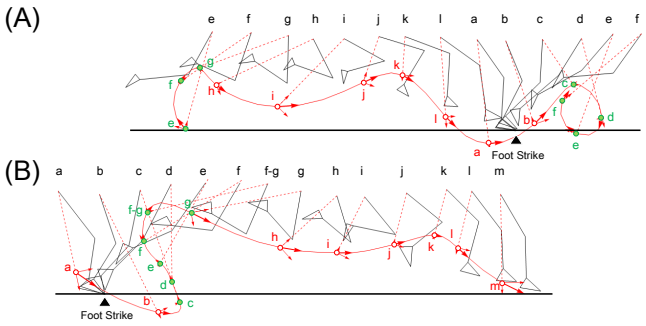

Fig. 5. Type-II virtual trajectory and kinematic posture. (A) a skilled child runner (representative participant A) and (B) a less-skilled child runner (representative participant D). The equilibria after foot-strike were regulated continuously, drawing the clockwise arc or circular trajectory with a moderate velocity (see also Fig. 1). The less-skilled runner showed a relatively slow equilibrium action response during the early swing phase. Note the additional gait phase (f-g) for the less-skilled runner.

indicate the data for the right and left legs, respectively. The red and blue markers represent the EP-based co-activation synergies for a skilled (participant A) (Fig. 3(A)) and a less-skilled child runner (participant D) (Fig. 3(B)), respectively. The gray markers represent the EP-based co-activation synergies of the other participants. A point in the ternary plot illustrates the three components of the EP-based co-activation synergies. Each component of the EP-based co-activation synergies represents the activity of the antagonistic muscle pair at which each A-A ratio, r_{h} (for hip), r_{hk} (for hip and knee), and r_{k} (for knee) contribute to the equilibrium.

B. Virtual trajectories

Figures 4 and 5 show the distinct types of virtual trajectories achieving similar kinematic sequences in the participants during sprinting. The type-I virtual trajectory in Fig. 4 was observed in one leg, and the type-II virtual trajectory in Fig. 5 was observed in the other leg for four of the five participants. Figures 4 (A) and 5(A) represent the virtual trajectory and kinematic posture for a skilled runner (participant A), while Figs 4(B) and 5(B) represent those of a less-skilled runner (participant D).

IV. DISCUSSION

A. EP-based co-activation synergies as common factors in children's sprints

The three components of EP-based co-activation synergies indicate the majority of activity for the muscles to be around the hip, hip and knee, and knee joints; these move in the radial, tangential, and null directions. The EP-based co-activation synergies $\boldsymbol{u}_R$ for radial movement were in the lower-left portion of the ternary plot (Fig. 3). This is reasonable because the knee muscles mainly contribute to endpoint movement in the radial direction. The EP-based co-activation synergies $\boldsymbol{u}_\Phi$ for tangential movement were located along the upper right axis of the ternary plot. This indicates that the hip muscles and hip-and-knee (bi-articular) muscles contribute to endpoint movement in the tangential direction. The EP-based co-activation synergies $\boldsymbol{u}_{null}$ for the modification of the mechanical impedance were located at the center of the ternary plot. All participants showed a similar distribution of EP-based synergies regardless of a skilled or less-skilled classification. However, some participants showed minor inter-limb differences in EP-based co-activation synergies within each portion of the ternary plot. These differences were unrelated to the classification of running skills. Thus, EP-based co-activation synergies could be regarded as common factors in the participants sprints.

B. Inter-limb asymmetry of equilibrium regulation for leg control

The virtual trajectory is defined in the configuration space of the EP-based co-activation synergies common to all the participants. The virtual trajectory during running always preceded the actual trajectory, showing a complicated path in the task space (Figs. 1, 4, and 5). Our results showed distinct virtual trajectory types for the right and left legs. In the type-I virtual trajectory, the equilibria after foot-strike were regulated intermittently during the early swing phase, quickly moving to a small space (ballpark) with a high velocity and remaining there (Fig. 4). In the type-II virtual trajectory, the equilibria after foot-strike were regulated continuously during the early swing phase, drawing an arc or circular trajectory with a moderate velocity (Fig. 5). An inter-limb asymmetry in equilibrium regulation for leg control was observed for participants A, B, D and E, while participant C showed a type-II virtual trajectory for both legs. One possible explanation for the inter-limb asymmetry is the effect of leg preference; one leg could be specialized for motion control (mobilization) under stable environmental conditions, and the other leg could be specialized for interactive control (balance) under unstable environmental conditions. We will seek the connection to motor lateralization that realizes the combination of motion and interactive control.

In general, movements are composed of two classes of primitive actions: rhythmic and discrete [16]. These are frequently considered motor primitives that are subserved by distinct neural or control mechanisms [17], [18]. This study investigated continuous repetitive movements that occur during sprinting, which is a typical rhythmic movement. However, our results suggested that the equilibria were discretely or intermittently regulated in one leg and continuously regulated in the other, thereby achieving similar kinematic postures during sprinting. These findings of inter-limb asymmetry of equilibrium regulation may provide insights into the interplay between the two fundamental movements.

Furthermore, the less-skilled sprinters (participants D and E) showed a slow equilibrium action response with an additional gait phase in both types of virtual trajectory during the early swing phase (Figs 4 and 5). The results suggest that the early swing phase is a crucial movement phase for skilled sprinting. Thus, the findings for equilibrium regulation could be beneficial for "tailor-made" coaching based on the types of leg control during sprinting.

In conclusion, this study highlights the counterintuitive control of lower limbs by children when they are sprinting; inter-limb asymmetry of equilibrium regulation achieves similar kinematic limb movement. The present study is limited by the number of participants (n=5) but further data collection and analysis on sprint performance in children of different ages and abilities could corroborate our findings on the effect of asymmetry in inter-limb equilibrium regulation. Information on gait asymmetry would be beneficial not only for coaching to improve sprint training but also from clinical and injury perspectives [19]. Our results may also contribute to the understanding of motor control problems in motor primitives [18] and support a speculative but promising training model based on a discrete or rhythmic or mechanical impedance aspect [20]. Our future work will examine mechanical intervention that will enable faster sprinting by children, based on our understanding of equilibrium regulation.

ACKNOWLEDGMENTS

We are grateful to Mr Yu Wadaki, an athletics instructor at Mizuno Sports Service Co., Ltd., for identifying the participants and evaluating their running performance. This study is based on his classification of running performance into skilled and less-skilled groups.

CONFLICT OF INTEREST

H. Hirai is a co-inventor of several Osaka University-held patents for EP-based co-activation synergy analysis.

REFERENCES

[1] J. B. Morin, M. Bourdin, P. Edouard, N. Peyrot, P. Samozino, and J. R. Lacour, "Machanical determinants of 100-m sprint running performance," *Eur. J. Appl. Physiol.*, vol. 112, no. 11, pp. 3921-3930, 2012.

[2] M. N. Dowson, M. E. Nevill, H. K. A. Lakomy, A. M. Nevill, and R. J. Hazeldine, "Modelling the relationship between isokinetic muscle strength and sprint running performance," *J. Sports Sci.*, vol. 16, no. 3, pp. 257-265, 1998.

[3] B. Schepens, P. A. Willems, and G. A. Cavagna, "The mechanics of running in children," *J. Physiol.*, vol. 509, no. 3, pp. 927-940, 1998.

[4] J. A. Mercer, J. S. Dufek, B. C. Magnus, M. D. Rubley, K. Bhanot, and J. M. Aldridge, "A description of shock attenuation for children running," *J. Athl. Train.*, vol. 45, no. 3, pp. 259-264, 2010.

[5] K. Seki, K. Suzuki, K. Yamamoto, A. Kato, M. Nakano, K. Aoyama, M. Ogata, and K. Kigoshi, "A study of leg recovery motion and sprint speed in male elementary school students: which motion should be learned, forward swing of the thigh or flexion of the knee in the recovery leg," *Japan J. Phys. Educ. Hlth. Sport Sci.*, vol, 61, no. 2, pp, 743-753, 2016. (in Japanese)

[6] F. Miyazaki, H. Hirai, M. Mitsunori, K. Uno and T. Oku, Motion analysis apparatus, method for analyzing motion, and motion analysis program, US20160324436A1, 2020.

[7] N. Bernstein, *The co-ordination and regulation of movements*, Oxford, Pergamon, 1967.

[8] A. O. Perotto, *Anatomical Guide for the Electromyographer: The Limbs and Trunk*, 5th edn., Springfield: Charles C Thomas Publisher, Ltd., 2011.

[9] E. Criswell, *Cram's Introduction to Surface Electromyography*, 2nd edn., Sudbury: Jones and Bartlett Publishers, 2011.

[10] D. Avers, and M. Brown, *Daniels and Worthingham's Muscle Testing: Techniques of Manual Examination and Performance Testing*, 10th edn., Saunders, 2018.

[11] H. Hirai, F. Fumio, H. Naritomi, K. Koba, T. Oku, K. Kanna, M. Uemura, T. Nishi, M. Kageyama, H. I. Krebs, "On the origin of muscle synergies: invariant balance in the co-activation of agonist and antagonist muscle pairs," *Front. Bioeng. Biotechnol.*, vol. 3, no. 192, 2015.

[12] H. Hirai, H. Pham, Y. Ariga, K. Uno, and F. Miyazaki, "Motor control based on the muscle synergy hypothesis," *Cognitive neuroscience robotics A: synthetic approaches to human understanding*, pp. 25-50, Springer, 2016.

[13] E. Watanabe, H. Hirai and H. I. Krebs, "Equilibrium point-based control of muscle-driven anthropomorphic legs reveals modularity of human motor control during pedalling," *Adv. Rob.*, vol. 34, no. 5, pp. 328-342, 2020.

[14] K. Hori, H. Hirai, D. Kogawa, H. Nagao, Y. Kaneko, R. Fujihara, S. Yamaguchi, T. Hikawa, K. Kozasa, N. Yamada, S. Yamamoto, K. Matsui, A. Nishikawa, and H. I. Krebs, "Coactivation synergies as physiological markers of locomotor skills in athletes," *Proc. 42nd Ann. Int. Conf. IEEE Eng. Med. Biol. Soc. (EMBC2020)*, 2230, 2020.

[15] D. Kogawa, H. Hirai, and H. Okamoto, "Classification of the runner's preferences in running shoes based on equilibrium-point-based muscle synergies," *Proceedings 2020 (Proc. 13th Conf. Int. Sports Eng. Assoc. (ISEA2020))*, vol. 49, no. 1, 85, 2020.

[16] N. Hogan and D. Sternad, "On rhythmic and discrete movements: reflections, definitions and implications for motor control," *Exp. Brain Res.*, vol. 181, no. 1, pp. 13-30, 2007.

[17] S. Schaal, D. Sternad, R. Osu, and M, Kawato, "Rhythmic arm movement is not discrete," *Nat. Neurosci.*, vol. 7, no. 10, pp. 1136-1143, 2004.

[18] N. Hogan and D. Sternad, "Dynamic primitives of motor behavior," *Biol. Cybern.*, vol. 106, no. 11-12, pp. 727-739, 2012.

[19] T. A. Exell, M. J. R. Gittoes, G. Irwin, and D. G. Kerwin, "Gait asymmetry: composite scores for mechanical analyses of sprint running," *J. Biomech.*, vol. 45, no. 6, pp. 1108-1111, 2012.

[20] T. Susko, K. Swaminathan, and H. I. Krebs, "MIT-skywalker: a novel gait neurorehabilitation robot for stroke and cerebral palsy," *IEEE Trans. Neural Syst. Rehabil. Eng.*, vol. 24, no. 10, pp. 1089-1099, 2016.